Dual-Based a posteriori Error Estimate for Stochastic Finite Element Methods

L. Mathelin [a,*] & O.P. Le Maître [b]

[a] *LIMSI-CNRS, BP 133, 91403 Orsay, France.*

[b] *LMEE and LIMSI-CNRS, Université d'Evry Val d'Essonne, 40 rue du Pelvoux, CE 1455, 91020 Evry, France.*

Abstract

We present an *a posteriori* error estimation for the numerical solution of a stochastic variational problem arising in the context of parametric uncertainties. The discretization of the stochastic variational problem uses standard finite elements in space and piecewise continuous orthogonal polynomials in the stochastic domain. The *a posteriori* methodology is derived by measuring the error as the functional difference between the continuous and discrete solutions. This functional difference is approximated using the discrete solution of the primal stochastic problem and two discrete adjoint solutions (on two imbricated spaces) of the associated dual stochastic problem. The dual problem being linear, the error estimation results in a limited computational overhead. With this error estimate, an adaptive refinement of the approximation space can be performed. The refinement can concern the spatial or stochastic approximations, and can consist in increasing the approximation order or in using finer elements. The efficiency of the proposed methodology is verified for the uncertain Burgers' equation using different refinement strategies.

Key words: error analysis, stochastic finite element method, uncertainty quantification, refinement scheme.

1 Introduction

Simulation of physical systems is often challenged by incomplete knowledge of model parameters, including initial conditions, boundary conditions, external

* Corresponding author. Tel: 33-169 85 80 69; fax: 33-169 85 80 88.
Email addresses: mathelin@limsi.fr (L. Mathelin), olm@iup.univ-evry.fr (O.P. Le Maître).

forcing, physical properties and modeling constants. In these situations, it is relevant to rely on a probabilistic framework and to consider the unknown model data as random quantities. Consequently, it becomes essential to assess the variability of the model solution induced by the variability of the model data, *i.e.* to propagate and quantify the impact of the uncertainty on the model solution. In a probabilistic framework, the uncertainty quantification consists in the determination of the probability law of the model solution induced by the probability law of the data, in order to establish confidence intervals, to estimate limits of predictability and/or to support model-based decision analysis.

Uncertainty propagation and quantification has recently received considerable attention, particularly through the development of efficient spectral techniques based on Polynomial Chaos (PC) expansions. PC based methods were originally developed for engineering problems in solid mechanics [10, 25] and subsequently applied to a large variety of problems, including flow through porous media [8, 9], thermal problems [12, 13], incompressible [15, 19, 30] and compressible flows [20, 21] (see also [14] for a review of recent developments in PC methods for fluid flows) and reacting systems [7, 24]. PC expansions consist in the representation of the uncertain data as functionals of a finite set of independent random variables with prescribed densities, the uncertainty germ, and in expanding the dependence the model solution using a suitable basis of uncorrelated functionals of the germs. A classic choice for the basis is a set of polynomials in the germ. If the germ has zero-mean normalized Gaussian components, one obtains the Wiener-Hermite PC basis [28, 5], which is formed of generalized Hermite polynomials. Other density types of the germ components result in various families of orthogonal polynomials or mixtures of orthogonal polynomials [29]. Two distinct types of solution methods can be used to compute the expansion coefficients of the stochastic solution: the sampling based approaches and the Galerkin projection. In the former type of methods, one solves a series of deterministic problems for different values of the uncertain model data and makes use of the resulting sample set of solutions to estimate the expansion coefficients (see for instance [24, 19]). The second type of methods, which is considered in the following, consists on the contrary in a projection of the model equations (weak formulation) on the expansion basis. This Galerkin projection results in a set of generally coupled deterministic problems for the stochastic modes of the solution.

Piecewise polynomials [27] and multi-wavelets [16, 17] were recently proposed as elements of the stochastic basis. These representations were developed to address the limitations of global spectral representations for complex, steep or even discontinuous dependencies of the model solution with regard to the data, for instance when a bifurcation appears for values of the data in the uncertainty domain. A key aspect of these discontinuous stochastic approximations is that they naturally offer flexibility for a local adaptation of the

representation to the solution. This adaptation allows for improvements of the computed solution, through local refinements of the approximation space, while maintaining the dimension of the representation basis and of the set of coupled problems to be solved at a reasonable level. The refinement of the stochastic approximation space can in fact consist in an increase of the local expansion order (p-refinement) or in using polynomials being continuous over smaller supports (h-refinement). For instance, in [16, 17] the domain of the random parameters is partitioned in sub-domains over which independent discontinuous low order expansions are employed. Heuristic criteria, based on the spectrum of the local expansion, is used to decide whether the local expansion is sufficient or whether it should be improved by means of h-refinement, *i.e.* by splitting the sub-domain into smaller ones, and along which dimension of the germ. A similar strategy is pursued in [27] but in the context of hp-spectral approximations. The refinement is also based on heuristic arguments involving the relative contribution of the higher order terms to the local solution expansion.

Although these schemes have been shown to provide significant improvements over global PC expansions, in terms of robustness (see for instance [18]) and computational efficiency, they still lack rigorous criteria for triggering the refinement. The objective of the present paper is therefore the derivation of a rigorous error estimator, to be used in place of the heuristic error indicators. To this end, we have decided to extend the dual-based *a posteriori* error technique commonly used in the (deterministic) finite element community. This choice was motivated by the firm and rigorous theoretical foundations of this error estimate technique, and because of its variational framework which makes it suitable for extension to the Galerkin projection of stochastic problems.

The paper is organized as follows. In Section 2, the variational formulation of a generic stochastic problem, based on a mathematical model involving parametric (data) uncertainties, is considered. The stochastic variational problem and construction of the approximation space are detailed. The latter involves a finite element discretization in space and a piecewise continuous approximation along the stochastic dimensions. In Section 3, the dual-based *a posteriori* error estimation is introduced. The methodology makes use of a differentiable functional to measure the difference between the exact (continuous) and approximated (discrete) stochastic solutions. Provided the discrete solution is sufficiently close to the continuous one, their functional difference is shown to be well approximated by a simple estimate. This estimate involves the discrete solutions of the primal and associated dual problems, and the continuous adjoint solution of the dual problem. A classic surrogate of the continuous adjoint solution is proposed, resulting in an error estimate methodology requiring the resolution of the discrete primal problem and two dual problems on different approximation spaces. The dual problems to be solved being linear, the computational overhead of the error estimator is expected to be limited. In

Section 4, we discuss the various strategies that can be subsequently used to improve the approximation in order to reduce the error. The reduction of the error can be performed by using smaller elements or by increasing the orders of the spatial and stochastic approximation spaces. As in the deterministic context, the determination of the optimal refinement strategy is an open question, which is made even more difficult and critical in the present stochastic context where the stochastic space (domain of the germ) may have many dimensions. Consequently, Section 5 presents some numerical tests aiming at showing the validity of the proposed dual-based error estimator in deciding which spatial/stochastic elements need priority refinement. The test problem is based on the 1-D Burgers' equation, with uncertainty on the viscosity and a boundary condition. Different algorithms of increasing complexity are proposed for the local refinement of the stochastic and spatial approximations, based on the dual-based error estimation. Finally, major findings of this work and few recommendations for future developments are summarized in Section 6.

2 Variational formulation of uncertain flow

2.1 Deterministic variational problem

We consider the standard variational problem for u on a M-dimensional domain $\Omega_x \subset \mathbb{R}^{\mathrm{M}}$ with homogeneous Dirichlet boundary condition ($u = 0$) on the boundary $\partial\Omega_x$ of Ω_x:

$$a(u;\varphi) = b(\varphi) \quad \forall \varphi \in \mathcal{V}_x, \tag{1}$$

to be solved for $u \in \mathcal{V}_x$, a suitable Hilbert space of Ω_x. In Eq. (1), a is a differentiable semi-linear form and b a linear functional.

2.2 Stochastic variational problem

It is assumed that the mathematical model given by Eq. (1) involves some parameters, or data, denoted by a real-valued vector d. The data may for instance consist of some physical constants involved in the model. Clearly, the solution u of the variational problem depends on the data value, a fact stressed by making explicit the dependence of the variational problem with d:

$$a(u;\varphi|d) = b(\varphi|d) \quad \forall \varphi \in \mathcal{V}_x. \tag{2}$$

If the actual value of the data d is not exactly known, *i.e.* if it is uncertain, it is suitable to consider d as a random quantity defined on an abstract probability

space $(\Theta, \mathcal{B}, dP)$, Θ being the set of elementary outcomes θ, $\mathcal{B}$ the σ-algebra of the events and dP a probability measure. In this context, the solution of the model is also random. In the following, we adopt the convention consisting in using uppercase letters to denote random quantities. Therefore, the random solution U and data D are dependent stochastic quantities defined on the same probability space $(\Theta, \mathcal{B}, dP)$; the dependency between U and D is prescribed by the model. Uncertainty propagation and quantification thus consists in the inference of the probability law of U, given the probability law of D and the mathematical model relating the two. It is assumed that the problem is well-posed in the sense that problem (2) has almost surely a unique solution.

We denote $\mathcal{V}_\Theta = L^2(\Theta, dP)$ the space of second order random variables. We thus have to solve, for $U \in \mathcal{V}_x \otimes \mathcal{V}_\Theta$,

$$A(U; \Phi|D) = B(\Phi|D) \quad \forall \Phi \in \mathcal{V}_x \otimes \mathcal{V}_\Theta, \tag{3}$$

where

$$A(U; \Phi|D) \equiv \int_\Theta a(U(\theta); \Phi(\theta)|D(\theta) dP(\theta), \quad B(\Phi|D) \equiv \int_\Theta b(\Phi(\theta)|D(\theta)) dP(\theta). \tag{4}$$

2.3 Stochastic discretization

We assume that D is parameterized as a functional of a finite number N of independent identically distributed real valued random variables ξ_i, defined on $(\Theta, \mathcal{B}, dP)$ with value in $S_\xi \subset \mathbb{R}$:

$$D = D(\xi), \quad \xi = (\xi_1, \ldots, \xi_{\mathrm{N}}) \in (S_\xi)^{\mathrm{N}} \equiv \Omega_\xi \subset \mathbb{R}^{\mathrm{N}}. \tag{5}$$

The vector ξ of random parameters is often referred to as the uncertainty germ. We denote p the known probability density function of ξ_i such that, by virtue of the independence, the joint distribution of ξ writes

$$p_\xi(\xi) = p_\xi(\xi_1, \ldots, \xi_{\mathrm{N}}) = \prod_{i=1}^{\mathrm{N}} p(\xi_i). \tag{6}$$

Without loss of generality, we shall restrict ourself in the following to germs having uniformly distributed components on $S_\xi = [-1, 1]$ and consequently we have

$$p(\xi_i) = \begin{cases} 1/2 & \text{if } \xi_i \in [-1, 1] \\ 0 & \text{otherwise} \end{cases}, \quad \Omega_\xi = [-1, 1]^{\mathrm{N}}. \tag{7}$$

Note however that the developments given below can be easily extended to the situation where the ξ_i have different ranges and/or different distributions.

The variational problem can be formulated in the image probability space $(\Omega_\xi, \mathcal{B}_\xi, p_\xi)$, using

$$\begin{aligned} A(U;\Phi|D) &= \int_\Theta a(U(\theta);\Phi(\theta)|D(\theta)\, dP(\theta) \\ &= \int_{\Omega_\xi} a(U(\xi);\Phi(\xi)|D(\xi)\, p_\xi(\xi) d\xi \equiv \langle a(U;\Phi|D)\rangle_{\Omega_\xi}\,, \end{aligned} \tag{8}$$

$$\begin{aligned} B(\Phi|D) &= \int_\Theta b(\Phi(\theta)|D(\theta))\, dP(\theta) \\ &= \int_{\Omega_\xi} b(\Phi(\xi)|D(\xi))\, p_\xi(\xi) d\xi \equiv \langle b(\Phi|D)\rangle_{\Omega_\xi}\,. \end{aligned} \tag{9}$$

Moreover, the stochastic functional space is now $\mathcal{V}_\xi = L^2(\Omega_\xi, p_\xi)$ and the variational problem becomes

$$A(U;\Phi|D) = B(\Phi|D) \quad \forall \Phi \in \mathcal{V}_x \otimes \mathcal{V}_\xi, \tag{10}$$

to be solved for $U \in \mathcal{V} \equiv \mathcal{V}_x \otimes \mathcal{V}_\xi$.

Following [27], we rely on piecewise orthogonal polynomials to construct the stochastic approximation space. The stochastic range Ω_ξ is divided into a collection of $\mathrm{N_b}$ non-overlapping sub-domains $\Omega_\xi^{(m)}$ referred to as stochastic elements (SEs) in the following. In this work, the SEs are hyper-rectangles:

$$\Omega_\xi = \bigcup_{m=1}^{\mathrm{N_b}} \Omega_\xi^{(m)}, \quad \Omega_\xi^{(m)} = [\xi_1^{(m),-}, \xi_1^{(m),+}] \times \cdots \times [\xi_\mathrm{N}^{(m),-}, \xi_\mathrm{N}^{(m),+}]. \tag{11}$$

On $\Omega_\xi^{(m)}$, the dependence of the data and solution with the random germ ξ is expressed as a truncated Fourier-like series,

$$U(\xi \in \Omega_\xi^{(m)}) = \sum_{k=0}^{\mathrm{P}(m)} u_k^{(m)} \Psi_k^{(m)}(\xi), \quad D(\xi \in \Omega_\xi^{(m)}) = \sum_{k=0}^{\mathrm{P}(m)} d_k^{(m)} \Psi_k^{(m)}(\xi), \tag{12}$$

where $\Psi_k^{(m)}(\xi)$ are orthogonal random polynomials in ξ and $u_k^{(m)}$, $d_k^{(m)}$ are the deterministic expansion coefficients over $\Omega_\xi^{(m)}$ of the solution and data respectively. The orthogonality of the random polynomials is defined with regards to the expectation over the respective SE. Denoting $\langle\cdot\rangle_{\Omega_\xi^{(m)}}$ the expectation over the m-th SE, the orthogonality of the polynomials writes:

$$\begin{aligned} \left\langle \Psi_k^{(m)} \Psi_{k'}^{(m)} \right\rangle_{\Omega_\xi^{(m)}} &= \frac{1}{\left|\Omega_\xi^{(m)}\right|} \int_{\Omega_\xi^{(m)}} \Psi_k^{(m)}(\xi)\, \Psi_{k'}^{(m)}(\xi)\, p_\xi(\xi)\, d\xi \\ &= \delta_{kk'} \left\langle {\Psi_k^{(m)}}^2 \right\rangle_{\Omega_\xi^{(m)}}, \end{aligned} \tag{13}$$

where

$$\left|\Omega_\xi^{(m)}\right| = \int_{\Omega_\xi^{(m)}} p_\xi(\xi)\, d\xi, \tag{14}$$

and $\delta_{kk'}$ is the usual Kronecker delta symbol. These polynomials vanish outside their respective support:

$$\Psi_k^{(m)}(\xi \notin \Omega_\xi^{(m)}) = 0 \quad \forall k = 0, \ldots, \mathrm{P}(m). \tag{15}$$

The number of terms $\mathrm{P}(m)$ in the expansions Eqs. (12) is a function of the selected stochastic expansion order $\mathrm{q}(m)$ of the SE:

$$\mathrm{P}(m) + 1 = \frac{(\mathrm{q}(m) + \mathrm{N})!}{\mathrm{q}(m)!\, \mathrm{N}!}. \tag{16}$$

The ξ_i being uniformly distributed, the polynomials $\Psi_k^{(m)}$ are simply rescaled and shifted multidimensional Legendre polynomials [1]. The stochastic approximation space is

$$\mathcal{V}_\xi^h = \mathrm{span}\left(\{\Psi_k^{(m)}\},\ 1 \leq m \leq \mathrm{N_b},\ 0 \leq k \leq \mathrm{P}(m)\right), \tag{17}$$

and the stochastic approximation can be improved by increasing the number $\mathrm{N_b}$ of SEs, *i.e.* through refinement of the partition of Ω_ξ, and/or by increasing the stochastic expansion order $\mathrm{q}(m)$ over some stochastic elements.

2.4 Finite element discretization

Consider a partition of Ω_x into a set of $\mathrm{N_x}$ non-overlapping finite elements (FE) with respective support $\Omega_x^{(l)}$ for $l = 1, \ldots, \mathrm{N_x}$:

$$\Omega_x = \bigcup_{l=1}^{\mathrm{N_x}} \Omega_x^{(l)}. \tag{18}$$

The FE approximation of the continuous solution U, denoted U^h, over the element $\Omega_x^{(l)}$ writes

$$U^h(x \in \Omega_x^{(l)}) = \sum_{i=1}^{\mathrm{N_d}(l)} U_i^{(l)} \mathcal{N}_i^{(l)}(x), \tag{19}$$

where $\mathrm{N_d}(l)$ is the number of degrees of freedom of the l-th element and $\mathcal{N}_i^{(l)}$ the associated spatial shape functions. We denote $\mathrm{p}(l)$ the polynomial order of the shape functions over $\Omega_x^{(l)}$. The spatial approximation space is thus

$$\mathcal{V}_x^h = \mathrm{span}\left(\{\mathcal{N}_i^{(l)}\},\ 1 \leq l \leq \mathrm{N_x},\ 1 \leq i \leq \mathrm{N_d}(l)\right), \tag{20}$$

and the spatial approximation can be improved by a refinement of the partition of the spatial domain Ω_x or by increasing the spatial order $\mathrm{p}(l)$ of some finite elements.

2.5 Approximation space $\mathcal{V}^h$

From the stochastic and spatial approximation spaces defined above, the approximation space $\mathcal{V}^h$ of the stochastic variational problem is seen to be:

$$\mathcal{V}^h = \mathcal{V}_x^h \otimes \mathcal{V}_\xi^h. \tag{21}$$

The solution at a point (x, ξ) of $\Omega \equiv \Omega_x \times \Omega_\xi$ has for expression:

$$U(x \in \Omega_x^{(l)}, \xi \in \Omega_\xi^{(m)}) = \sum_{i=1}^{\mathrm{N_d}(l)} \sum_{k=0}^{\mathrm{P}(m)} u_{i,k}^{(l,m)} \, \mathcal{N}_i^{(l)}(x) \, \Psi_k^{(m)}(\xi), \tag{22}$$

where the deterministic coefficient $u_{i,k}^{(l,m)}$ is the k-th uncertainty mode of the m-th SE for the i-th degree of freedom of the l-th FE.

An immediate consequence of the tensored construction of the approximation space $\mathcal{V}^h$ is that the spatial FE discretization is the same for all the stochastic elements $\Omega_\xi^{(m)}$, and conversely the stochastic discretization is the same for all spatial finite elements $\Omega_x^{(l)}$. This is clearly not optimal as some portions of the stochastic domain Ω_ξ may require finer spatial discretization than others to achieve a similar accuracy. Conversely, the solution in some parts of spatial domain Ω_x may exhibit more complex dependences with regards to $D(\xi)$, therefore requiring a finer stochastic discretization than at other locations. However, for the tensored construction $\mathcal{V}^h$, the discrete solution can be improved through a) refinement of the FE approximation space $\mathcal{V}_x^h$ uniformly over Ω_ξ, and b) refinement of the stochastic approximation space $\mathcal{V}_\xi^h$ uniformly over Ω_x.

In fact, this symmetric situation can be easily relaxed: an adaptation to each SE of the spatial discretization, *i.e.* the number of elements $\mathrm{N_x}$ and/or the number of degrees of freedom of the elements $\mathrm{N_d}$, causes no difficulty. This is due to the complete independence of the solution over different stochastic elements, a feature emerging from the absence of any differential operator along the uncertainty dimensions. Consequently, the adaptation of $\mathcal{V}_x^h$ with the SEs was actually implemented and used for the generation of the results presented hereafter. However, to simplify the presentation of the method and the notation, this feature is not detailed here. On the other hand, using a variable stochastic approximation for different spatial FE is much more cumbersome and remains to be investigated. This adaptation would require the

development of non-obvious matching conditions of the stochastic approximation across FE boundaries.

3 Dual-based *a posteriori* error estimate

3.1 a posteriori error

We adopt the convention that the functionals are linear with respect to arguments placed on the right-side of a semicolon. For a finite dimensional subspace $\mathcal{V}^h \subset \mathcal{V}$, the discretized solution $U^h \in \mathcal{V}^h$ is the Galerkin approximation defined as the solution of the discrete problem

$$A(U^h; \Phi^h | D^h) = B(\Phi^h | D^h) \quad \forall \Phi^h \in \mathcal{V}^h. \tag{23}$$

Let $\mathscr{J} : \Omega \to \mathbb{R}$ be a differentiable functional of the solution. In the spirit of [3] and [2] among others, one is interested in approximating $\mathscr{J}(U)$ as closely as possible by $\mathscr{J}(U^h)$, *i.e.* to minimize the difference $\mathscr{J}(U) - \mathscr{J}(U^h)$ in some sense. We seek for an expression of $\mathscr{J}(U) - \mathscr{J}(U^h)$. To this end, let us define the Lagrangian $\mathscr{L}$ of the continuous solution by:

$$\mathscr{L}(U; Z) \equiv \mathscr{J}(U) + B(Z|D) - A(U; Z|D), \tag{24}$$

where $Z \in \mathcal{V}$ is the adjoint variable of the continuous problem. The adjoint variable Z is a Lagrange multiplier of the optimization problem for the minimization of $\mathscr{J}(U)$ under the constraints of Eq. (10). Formally, this minimum corresponds to the stationary points of $\mathscr{L}$:

$$\frac{\partial \mathscr{L}}{\partial U} = \mathscr{J}'(U; \Phi') - A'(U; \Phi', Z|D) = 0 \quad \forall \Phi' \in \mathcal{V}, \tag{25}$$

$$\frac{\partial \mathscr{L}}{\partial Z} = B(\Phi|D) - A(U; \Phi|D) = 0 \quad \forall \Phi \in \mathcal{V}. \tag{26}$$

Eq. (25) is the adjoint (or dual) problem, while Eq. (26) is the state (or primal) problem. Note that the derivatives are in the Gâteaux sense:

$$\mathscr{J}'(U; \Phi') = \lim_{\varepsilon \to 0} \frac{\mathscr{J}(U + \varepsilon\, \Phi') - \mathscr{J}(U)}{\varepsilon},$$

$$A'(U; \Phi', Z|D) = \lim_{\varepsilon \to 0} \frac{A(U + \varepsilon\, \Phi'; Z|D) - A(U; Z|D)}{\varepsilon}.$$

The discrete counterpart of the dual and primal problems are in turn

$$\mathscr{J}'(U^h;\Phi^{h'}) - A'(U^h;\Phi^{h'},Z^h|D^h) = 0 \quad \forall \Phi^{h'} \in \mathcal{V}^h, \tag{27}$$

$$B(\Phi^h|D^h) - A(U^h;\Phi^h|D^h) = 0 \quad \forall \Phi^h \in \mathcal{V}^h. \tag{28}$$

Combining these results, one obtains

$$\begin{aligned}\mathscr{L}(U,Z) - \mathscr{L}(U^h,Z^h) &= \mathscr{J}(U) + B(Z) - A(U;Z) - \mathscr{J}(U^h) - B(Z^h) \\ &\quad + A(U^h;Z^h) \\ &= \mathscr{J}(U) - \mathscr{J}(U^h),\end{aligned} \tag{29}$$

where the dependences of A and F on D have been dropped to simplify the notations. It is seen from Eq. (29) that the difference in $\mathscr{J}$ for the continuous and discrete solutions is equal to the difference in their respective Lagrangian.

3.2 A posterior error estimation

Following [4], among others, we now derive a more practical expression for the difference $\mathscr{J}(U) - \mathscr{J}(U^h)$. Let $K(\cdot)$ be a differentiable functional on a given functional space $\mathcal{W}$. The difference $K(v) - K(v^h)$, for v and $v' \in \mathcal{W}$, can be expressed as an integral between v and v^h of the derivative of K:

$$K(v) - K(v^h) = \int_{v^h}^{v} K'(v')\, dv'. \tag{30}$$

The integration path can be parameterized to obtain

$$\begin{aligned}K(v) - K(v^h) &= \int_0^1 K'(v^h + s\,(v - v^h))\,(v - v^h)\, ds \\ &= \int_0^1 K'(v^h + s\,e_v; e_v)\, ds,\end{aligned} \tag{31}$$

where $e_v \equiv v - v^h$. Here, use was made again of the convention regarding the linearity of the functional forms with regard to the arguments on the right-side of the semicolon. Using $K'(v) = 0$, the right-hand side of Eq. (31) can be rewritten as

$$K(v) - K(v^h) = \int_0^1 K'(v^h + s e_v; e_v) ds + \frac{1}{2}\left[K'(v^h; e_v) - K'(v^h; e_v) + K'(v; e_v)\right]. \tag{32}$$

Making use of the Galerkin orthogonality and the trapezoidal rule it comes

$$K(v) - K(v^h) = \frac{1}{2}K'(v^h; e_v) + \frac{1}{2}\int_0^1 K^{(3)}(v^h + s\,e_v; e_v^3)\, s\,(s-1)\, ds. \tag{33}$$

Applying this relation to the difference of the Lagrangian of the continuous and discrete solutions leads, after some algebra, to:

$$\mathscr{J}(U) - \mathscr{J}(U^h) = \frac{1}{2}\left[\rho(U^h, Z - \Phi'^h) + \rho^*(Z^h, U - \Phi^h)\right] + \widetilde{R}, \tag{34}$$

with the residuals

$$\rho(U^h, \cdot) \equiv B(\cdot) - A(U^h; \cdot), \tag{35}$$
$$\rho^*(Z^h, \cdot) \equiv \mathscr{J}'(U^h, \cdot) - A'(U^h; \cdot, Z^h). \tag{36}$$

The remainder term $\widetilde{R}$ in Eq. (34) has for expression

$$\begin{aligned}\widetilde{R} = \frac{1}{2}\int_0^1 \Big[& \mathscr{J}^{(3)}(U^h + s\,E_U; E_U^3) - A^{(3)}(U^h + s\,E_U; E_U^3, Z^h + s\,E_Z) \\ & -3\,A''\,(U^h + s\,E_U; E_U^2\,E_Z)\Big]\; s\,(s-1)\,ds,\end{aligned} \tag{37}$$

with the error terms defined as $E_U = U - U^h$ and $E_Z = Z - Z^h$. Thus $\widetilde{R}$ is cubic in the error, suggesting that it can be neglected provided that the continuous and discrete solutions are sufficiently close. It is also seen that the residuals are functional of both the primal and dual continuous solutions U and Z, such that using Eq. (34) to estimate $\mathscr{J}(U) - \mathscr{J}(U^h)$ would require two surrogates of U and Z even if $\widetilde{R}$ is neglected. In fact, the expression can be further simplified to remove the contribution of U. Using an integration by part of $\widetilde{R}$, one obtains [4]

$$\rho^*(Z^h, U - \Phi^h) = \rho(U^h, Z - \Phi'^h) + \Delta\rho, \tag{38}$$

where

$$\Delta\rho = \int_0^1 \left[A''(U^h + sE_U; E_U^2, Z^h + sE_Z) - \mathscr{J}''(U^h + sE_U; E_U^2)\right] ds. \tag{39}$$

Introducing this result into Eq. (34) leads to the final expression for the approximation error:

$$\mathscr{J}(U) - \mathscr{J}(U^h) = \rho(U^h, Z - \Phi'^h) + r, \tag{40}$$

where

$$r = \int_0^1 \left[A''(U^h + sE_U; E_U^2, Z) - \mathscr{J}''(U^h + sE_U; E_U^2)\right]\; s\,ds. \tag{41}$$

The remainder term r is now quadratic in E_U and will be neglected hereafter, assuming again that the discrete solution U^h is indeed a sufficiently close approximation of U.

At this point we have an estimate of the approximation error given by

$$\mathscr{J}(U) - \mathscr{J}(U^h) \approx B(Z - Z^h|D^h) - A(U^h; Z - Z^h|D^h), \tag{42}$$

where we have substituted Φ'^h by the adjoint solution of the discrete problem in Eq. (40), as usual in *a posteriori* error methodology. To evaluate this estimate, one needs to know the solutions U^h and Z^h of the primal and dual discrete problems and the solution Z of the continuous dual problem given by Eq. (25). However, the continuous dual problem can not be solved as it requires the knowledge of the exact solution U. Instead, a surrogate of Z denoted $\widetilde{Z}$ is used. This surrogate is classically constructed by solving a discrete dual problem on a refined finite dimensional space $\mathcal{V}^{\widetilde{h}}$ containing $\mathcal{V}^h$. The methodology is thus the following. Given an approximation space $\mathcal{V}^h$ we solve the primal and dual problems Eqs. (28,27) for U^h and $Z^h \in \mathcal{V}^h$. The refined space $\mathcal{V}^{\widetilde{h}} \supset \mathcal{V}^h$ is constructed by increasing the polynomial orders of both the approximation space $\mathcal{V}_x^h$ and $\mathcal{V}_\xi^h$, and we solve the following dual problem for $\widetilde{Z} \in \mathcal{V}^{\widetilde{h}}$

$$\mathscr{J}'(U^h; \Phi) - A'(U^h; \Phi, \widetilde{Z}|D^{\widetilde{h}}) = 0 \quad \forall \Phi \in \mathcal{V}^{\widetilde{h}}. \tag{43}$$

It yields the *a posteriori* error estimate given by

$$\mathscr{J}(U) - \mathscr{J}(U^h) \approx B(\widetilde{Z} - Z^h|D^h) - A(U^h; \widetilde{Z} - Z^h|D^h). \tag{44}$$

Two important remarks are necessary at this point. First, it is underlined that the dual problems are linear and significantly less expansive to solve than the primal problems, even in an enriched approximation space. Second, as shown by Eq. (43), the adjoint solution $\widetilde{Z}$ is based on a functional form A' constructed with the approximation of D on the enriched space $\mathcal{V}^{\widetilde{h}}$. As a consequence, the resulting error estimate based on $\widetilde{Z}$ accounts for possible error in the approximation of the uncertain data $D(\xi)$ on $\mathcal{V}_\xi^h$.

4 Refinement procedures

4.1 Global and local error estimates

The *a posteriori* error methodology described in section 3 gives access to an estimate of $\mathscr{J}(U) - \mathscr{J}(U^h)$ according to Eq.(44). The global approximation error η is therefore:

$$\begin{aligned}\eta &= \left|A(U^h;\widetilde{Z}-Z^h|D^h)-B(\widetilde{Z}-Z^h|D^h)\right| \\ &= \left|\left\langle a(U^h;\widetilde{Z}-Z^h|D^h)-b(\widetilde{Z}-Z^h|D^h)\right\rangle_{\Omega_\xi}\right| \\ &\leq \sum_{m=1}^{\mathrm{N_b}} \left|\Omega_\xi^{(m)}\right| \left|\left\langle a(U^h;\widetilde{Z}-Z^h|D^h)-b(\widetilde{Z}-Z^h|D^h)\right\rangle_{\Omega_\xi^{(m)}}\right| \end{aligned} \tag{45}$$

Defining the local error on the element $\Omega_x^{(l)} \times \Omega_\xi^{(m)}$ by

$$\eta_{l,m} \equiv \left| \int_{\Omega_\xi^{(m)}} \int_{\Omega_x^{(l)}} \left[\widetilde{a}(U^h;\widetilde{Z}-Z^h|D^h)-\widetilde{b}(\widetilde{Z}-Z^h|D^h)\right]\, p_\xi(\xi)\, dx\, d\xi \right|, \tag{46}$$

where

$$\int_{\Omega_x} \widetilde{a}(u;v|d)dx = a(u;v|d), \quad \int_{\Omega_x} \widetilde{b}(v|d)dx = b(v|d),$$

we obtain the following inequality:

$$\eta \leq \sum_{l=1}^{\mathrm{N_x}} \sum_{m=1}^{\mathrm{N_b}} \eta_{l,m}. \tag{47}$$

Then, the objective is to refine the approximation space $\mathcal{V}^h$ in order to reduce the global error η as estimated from the *a posteriori* error analysis. A popular strategy to ensure that the global error gets below a given threshold value ϵ_η is to refine the approximation such that

$$\eta_{l,m} < \frac{\epsilon_\eta}{\mathrm{N_x N_b}} = \epsilon, \quad \forall l,m \in [1,\mathrm{N_x}] \times [1,\mathrm{N_b}]. \tag{48}$$

4.2 Refinement strategies

If the criterion given in Eq.(48) is not satisfied for at least one SFE, the approximation space needs refinement. Different types of refinements are possible. First, from the tensored construction of the approximation space, $\mathcal{V}^h = \mathcal{V}_x^h \otimes \mathcal{V}_\xi^h$, it is seen that the refinement may concern the spatial or stochastic approximation spaces, or both. To distinguish these two types of refinement we shall refer in the following to x and ξ-refinement for the spatial and stochastic refinements respectively. Second, the refinement can be based on construction of finer partitions of the domains or on increased approximation orders, hereafter referred to as h- and p-refinements respectively. Therefore, we can choose between four fundamental types of refinements to reduce the approximation error to satisfy Eq. (48), h_ξ-, h_x-, p_ξ- or p_x-refinements, or any combination of the four.

The problem is thus to find the refinement strategy that yields the largest decay of the discretization error for the lowest computational cost. The difficulty

here is that the local error estimate only provides some information about the elements (SEs and FEs) over which the approximation is insufficient. In other words, if for some l and m the local error is such that $\eta_{l,m} > \epsilon$ then we can only safely consider that the approximation error over $\Omega_\xi^{(m)} \times \Omega_x^{(l)}$ is too large but nothing more. Specifically, it is not possible to decide a) between h- or p-refinement and b) whether one should enrich the approximation space $\mathcal{V}_x^h$ or $\mathcal{V}_\xi^h$.

Difficulty a) is a classic problem in (deterministic) hp-finite-element methods. In the deterministic context, different strategies have been proposed to support the decision regarding h- or p-refinement, and most of these strategies are based on trial approaches. For instance, in [11], a systematic trial of h-refinement is performed. The efficiency of the h-refinement is subsequently measured by comparing the resulting error reduction with its theoretical value estimated using the convergence rate of the FE scheme. If the efficiency of the h-refinement is not satisfactory, a p-refinement is enforced at the following refinement step. This type of trial/verification approach has not been retained here because of its numerical cost. Difficulty b) is on the contrary specific to stochastic finite-element methods and thus remains entirely to be investigated. A possible way to deal with difficulty b) can be envisioned again by a trial approach where one would apply successively x and ξ-refinements to measure the respective effectiveness in error reduction. Again, trial approaches are expected to be overly expensive in the stochastic context where the size of the discrete problems to be solved can be many times larger than for the deterministic case: better approaches, yet to be thought, are needed here.

Another issue arising in the stochastic context is the potentially large dimensionality N of the stochastic domain Ω_ξ: an isotropic h_ξ-refinement, where SEs are broken into smaller ones along each dimension ξ_i, can quickly result in a prohibitively large number of SEs. This issue was already observed in [16, 17, 18] where adaptive multi-wavelet approximations are used. Rather, it is desirable to gain further information on the structure of the local error $\eta_{l,m}$ in order to refine along the error's principal directions solely. Several approaches may be thought of to deal with this constraint. In the context of deterministic finite element method, several anisotropic error estimators have been rigorously derived based on higher order information. Among others, [23] and [22] use the Hessian matrix based on Clément interpolants [6] to derive an estimate of the directional errors. Thought attractive, this method has only been derived for first-order finite elements (P1) and its extension to higher order remains largely an open problem. This limitation precludes its use in the present context where approximation order q is routinely larger than one.

Considering all these difficulties, it was decided to first verify the effectiveness of the dual-based *a posteriori* error estimation in indicating which elements need refinement, and to delay the question of the refinement strategy decision

to a future work. Consequently, we present in a next section some numerical tests which essential purposes are to prove that the proposed error estimator indeed detect areas of Ω where the error is the most significant. Still, we perform refinements, of increasing complexity, without pretending in any way that the decision algorithms used yield optimal approximation spaces, but merely that they allow for a reduction of the global error to an arbitrary small level.

5 Numerical examples

5.1 Uncertain Burgers' equation

To test the *a posteriori* error estimator, we consider the 1-D Burgers' equation on the spatial domain $\Omega_x \in [x^-, x^+]$:

$$\begin{cases} \dfrac{1}{2}\,\left(u\,(1-u)\right)_x - \mu\,u_{xx} = 0 \quad \forall x \in [x^-, x^+], \\ u(x^-) = u^-, \quad u(x^+) = u^+. \end{cases} \tag{49}$$

This equation is widely used in particular in the fluid dynamics community as it features essential ingredients: diffusion as well as a quadratic convective term. Depending on the boundary conditions, the solution of the Burgers' equation exhibits areas where $u(x)$ is nearly constant and equal to u^- (for $x \simeq x^-$) and u^+ (for $x \simeq x^+$) with a central area, the transition layer, where u quickly evolves from u^- to u^+ according to an hyperbolic tangent profile having an increasing steepness with decreasing the fluid viscosity.

5.1.1 Uncertainty settings

We consider the random solution $U(x, \xi)$ of the Burgers' equation which arises when the viscosity μ is uncertain and parameterized by the random vector ξ: $\mu = \mu(\xi)$. As discussed above, ξ is uniformly distributed in $[-1, 1]^{\mathrm{N}}$. The number N of random variables depends on the parameterization. To ensure the existence of a solution to the stochastic problem, the parameterization is selected such that the viscosity is almost surely positive. The stochastic Burgers' equation is thus:

$$\begin{cases} \dfrac{1}{2}\,\left[U(x,\xi)\,(1-U(x,\xi))\right]_x - \mu(\xi)\,U_{xx}(x,\xi) = 0 \quad \forall x \in [x^-, x^+], \\ U(x^-,\xi) = u^-, \quad U(x^+,\xi) = u^+. \end{cases} \tag{50}$$

The viscosity is parameterized using N = 2 random variables as follows

$$\mu(\xi) = \mu_0 + \mu_1\xi_1 + \mu_2\xi_2, \quad \mu_0 > 0. \tag{51}$$

The expectation of the viscosity is $\langle\mu\rangle_{\Omega_\xi} = \mu_0$, and provided that $|\mu_1| + |\mu_2| < \mu_0$, $\mu(\xi)$ is almost surely positive. We shall set in the following $\mu_0 = 1$, $\mu_1 = 0.62$ and $\mu_2 = 0.36$. The resulting probability density function (pdf) of the random viscosity is plotted in Figure 1.

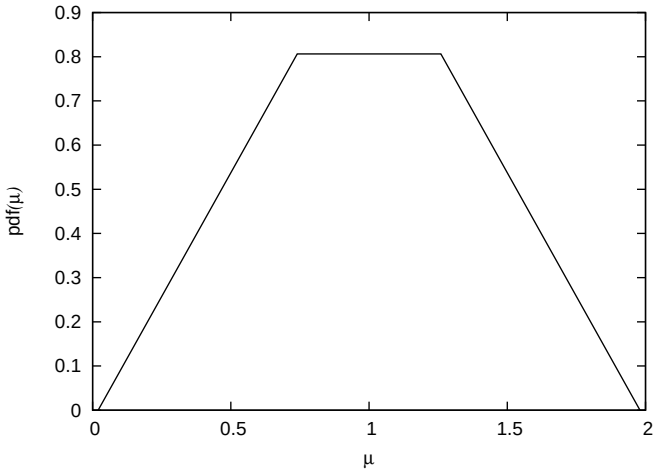

Fig. 1. Probability density function of the viscosity.

Finally, we set $x^- = -10$ and $x^+ = 10$ and we use for the boundary conditions,

$$u^- = \frac{1}{2}\left[1 + \tanh\left(\frac{x^-}{4\,\mu_0}\right)\right] \approx 0, \quad u^+ = \frac{1}{2}\left[1 + \tanh\left(\frac{x^+}{4\,\mu_0}\right)\right] \approx 1. \tag{52}$$

For these boundary conditions,

$$u(x) = \frac{1}{2}\left[1 + \tanh\left(\frac{x}{4\,\mu_0}\right)\right],$$

is in fact solution of the deterministic Burgers' equation for $\mu = \mu_0$ [26].

5.1.2 Variational problems

The variational formulation of the Burgers' equation is derived. By means of integration by parts, one obtains for the primal problem to be solved for $U \in \mathcal{V}$:

$$A(U;\Phi|D) - B(\Phi|D) = \left\langle \int_{\Omega_x} \left[U(1-U) - 2\,\mu\,U_x\right]\,\Phi_x\,dx \right\rangle_{\Omega_\xi} = 0 \quad \forall\Phi \in \mathcal{V}^*, \tag{53}$$

where $\mathcal{V}^* = \mathcal{V}_x^* \otimes \mathcal{V}_\xi$ is constructed using the restriction of $\mathcal{V}_x$ to functions vanishing on $\partial\Omega_x$. For the derivation of the adjoint problem, an obvious choice

is here to base the *a posteriori* error estimate on the solution itself, *i.e.* using

$$\mathscr{J}(U) = \left\langle \int_{\Omega_x} U \, dx \right\rangle_{\Omega_\xi} . \tag{54}$$

For this choice, we have

$$\mathscr{J}'(U;\Phi') = \lim_{\varepsilon\to 0} \frac{\mathscr{J}(U+\varepsilon\,\Phi') - \mathscr{J}(U)}{\varepsilon} = \left\langle \int_{\Omega_x} \Phi' \, dx \right\rangle_{\Omega_\xi} \quad \forall \Phi' \in \mathcal{V}. \tag{55}$$

and

$$A'(U,\Phi';Z|D) = \lim_{\varepsilon\to 0} \frac{A(U+\varepsilon\,\Phi';Z|D) - A(U;Z|D)}{\varepsilon} \tag{56}$$

$$= \left\langle \int_{\Omega_x} \left[(1-2\,U)\,Z_x\,\Phi' - 2\,\mu\,Z_x\,\Phi'_x\right] \, dx \right\rangle_{\Omega_x} . \tag{57}$$

Thus the dual problem writes as

$$\left\langle \int_{\Omega_x} \left[(1-2\,U)\,Z_x\,\Phi' - 2\,\mu\,Z_x\,\Phi'_x + \Phi'\right] \, dx \right\rangle_{\Omega_x} = 0 \quad \forall \Phi' \in \mathcal{V}, \tag{58}$$

for $Z \in \mathcal{V}$ and deterministic boundary conditions $Z(x^-) = Z(x^+) = 0$.

For the discretization of the primal and dual problems, we use Chebyshev finite elements to construct $\mathcal{V}_x^h$, and Legendre polynomials (uniform distribution) for $\mathcal{V}_\xi^h$ [1]. To compute the surrogate of the exact solution of the adjoint equation, the approximation $\mathcal{V}^h$ is extended to $\mathcal{V}^{\widetilde{h}}$ by increasing the orders of the Chebyshev and Legendre polynomials by one unit, as explained in Section 3. In practice, this step is cheap due to the linearity of the dual problem, as seen from Eq. (58), and the resolution of the dual problem only contributes to a small fraction of the global CPU time.

A fundamental point is that primal and dual problems do not involve any operator in the stochastic directions (derivatives in ξ_i) but in the spatial direction x solely. This has the essential implication that realizations of the Burgers' flow for different realizations of the viscosity are fully independent. As a result, the solution of the primal and dual problems over different SEs are uncoupled, allowing for straightforward parallelization with drastic speed-up of the computation. We took advantage of this characteristic by solving SE-wise the primal and dual problems on a Linux-cluster having 4 nodes with dual processors. Another interesting property of the stochastic decoupling between SEs is that, during the refinement process, the approximation needs only to be updated for the stochastic sub-domains $\Omega_\xi^{(m)}$ that have been x or ξ-refined.

In a first series of tests, the spatial discretization if held fixed with $\mathrm{N_x} = 6$ Chebyshev finite elements having equal size and order $\mathrm{p} = 6$. For the refinement, only h_ξ-refinement is allowed here while the stochastic order is maintained to a constant value.

For the purpose of comparison, we show in Figure 2 the convergence of the error in the computed mean and variance of U at the point $x = 0.52$ when the partition of Ω_ξ is *uniformly* refined by increasing the number $\mathrm{N_b}$ of SEs from 2^2 to 100^2. The mean and variance have for expression:

$$\begin{aligned} \left\langle U^h \right\rangle_{\Omega_\xi} &= \sum_{m=1}^{\mathrm{N_b}} \left|\Omega_\xi^{(m)}\right| \left\langle U^h \right\rangle_{\Omega_\xi^{(m)}}, \\ \sigma^2(U) \equiv \left\langle \left[U^h - \left\langle U^h \right\rangle_{\Omega_\xi} \right]^2 \right\rangle_{\Omega_\xi} &= \sum_{m=1}^{\mathrm{N_b}} \left|\Omega_\xi^{(m)}\right| \left\langle \left[U^h - \left\langle U^h \right\rangle_{\Omega_\xi} \right]^2 \right\rangle_{\Omega_\xi^{(m)}}. \end{aligned} \quad (59)$$

In this experiment, the SEs are squares with equal size. To estimate the errors, surrogates of the exact mean and variance of U were computed using $\mathrm{N_x} = 6$, $\mathrm{p} = 6$, $\mathrm{N_b} = 128^2$ and $\mathrm{q} = 6$. Note that these surrogates are in fact approximations of the exact mean and variance of the *semi-continuous* problem, the spatial discretization being held fixed. Consequently, it is not expected that the *a posteriori* error estimate η goes to zero since a small but finite spatial error persists even for $\mathcal{V}_\xi^h \to \mathcal{V}_\xi$. The plot in Figure 2 shows the convergence of the errors on the mean and variance at $x = 0.52$ of the semi-continuous solution for two stochastic orders $\mathrm{q} = 2$ and $\mathrm{q} = 4$. The error is seen to quickly decrease as the number of SEs increases, illustrating the convergence of the solution process. The errors on the mean and variance converge with a similar rate which is function of the stochastic order q.

However, it is known that this uniform refinement is not optimal, since some areas of Ω_ξ may require a finer discretization than others. Thus, instead of employing a uniform refinement, we now use the *a posteriori* error estimate to identify the SEs requiring refinement. Following Eq. (48), an h_ξ-refinement is to be performed on a SE $\Omega_\xi^{(m)}$ whenever $\eta_{l,m} \geq \epsilon$ for some $l \in [1, \mathrm{N_x} = 6]$. If so, the refinement consists in splitting $\Omega_\xi^{(m)}$ into $2^{\mathrm{N}} = 4$ smaller SEs of equal size (*i.e.* isotropically). Applying this scheme for $\mathrm{q} = 2$ gives the evolution with the refinement iterations of the errors in the computed mean and variance of U^h at $x = 0.52$ reported in Figure 3. These results were generated using $\epsilon = 2.10^{-5}$. The errors are plotted as a function of the total number of dual and primal problems actually solved during the iterative refinement process. The evolution of the errors for the uniform refinement previously shown in Figure 2 is also reported for comparison. A dramatic improvement of the convergence of the

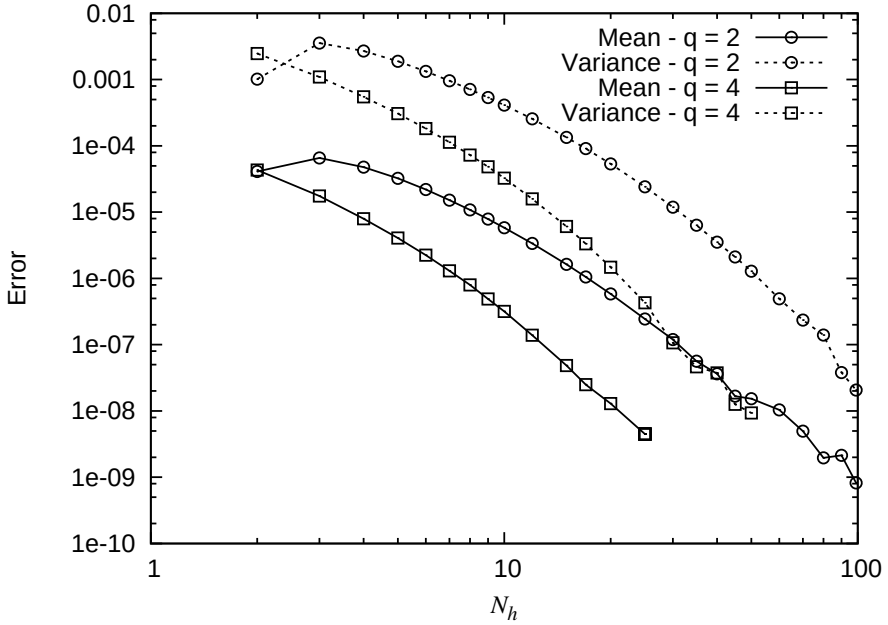

Fig. 2. Evolution of the errors on the computed (semi-continuous) mean and variance of the solution at $x = 0.52$ as a function of $N_h = \sqrt{\mathrm{N_b}}$ when using uniform h_ξ-refinement. Two stochastic orders q = 2 and q = 4 are reported as indicated.

errors on the two first moments is observed when the *a posteriori* error based refinement scheme is used, compared to the uniform refinement. Specifically, an error of $\sim 10^{-7}$ in the (semi-continuous) mean and variance is achieved at a cost of roughly 128 resolutions of the primal and dual problems when using the adaptive h_ξ-refinement, while about 5000 primal problems have to be solved to reach a similar accuracy when using a uniform refinement. Clearly, the adaptive h_ξ-refinement out-performs the uniform refinement, not only in terms of CPU-cost, but also in terms of memory requirements.

A better appreciation of the performance of the adaptive h_ξ-refinement can be gained from the analysis of the data reported in Table 1, which presents the evolution of the number $\mathrm{N_b}$ of SEs, the number of resolutions of primal and dual problems and the errors in the first two moments as the refinement proceeds. Starting from a partition of Ω_ξ into 4 equal SEs, they are first all refined along the two-directions ξ_1 and ξ_2 leading to a partition involving 16 SEs. At the second iteration, all these SEs are still considered too coarse to match the prescribed accuracy and are refined again in the two stochastic directions, resulting in 64 SEs. After the third iteration, only a fraction of the SEs needs further refinement and the process eventually stops after 6 iterations with a partition of the stochastic space into 97 SEs.

In a second series of test, the *a posteriori* error based isotropic h_ξ-refinement is applied with different stochastic orders q. The refinement criterion ϵ is increased to 5.10^{-5} while other numerical parameters are kept constant (*e.g.*

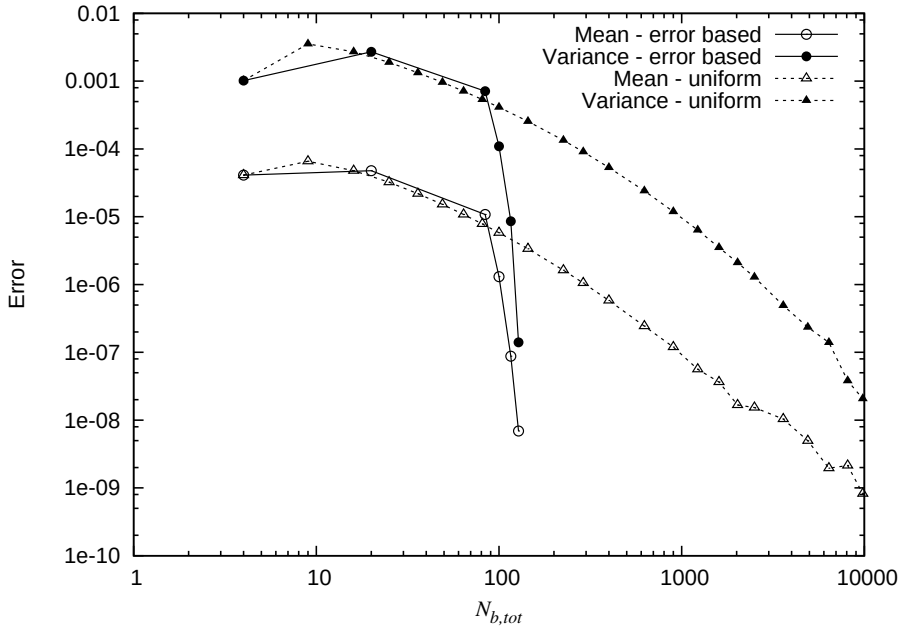

Fig. 3. Evolutions of the errors in computed (semi-continuous) mean and variance of the solution at $x = 0.52$ as a function of the number of primal and dual problems solves during the isotropic h_ξ-refinement and q = 2. Also plotted are the evolutions of the errors for the uniform refinement.

Iteration	N_b	# of resolutions	error on mean	error on variance
1	4	4	$4.1074\ 10^{-5}$	$1.0189\ 10^{-3}$
2	16	20	$4.7861\ 10^{-5}$	$2.7054\ 10^{-3}$
3	64	84	$1.0813\ 10^{-5}$	$7.1067\ 10^{-4}$
4	76	100	$1.3056\ 10^{-6}$	$1.0944\ 10^{-4}$
5	88	116	$8.7892\ 10^{-8}$	$8.5915\ 10^{-6}$
6	97	128	$6.9087\ 10^{-9}$	$1.4032\ 10^{-7}$

Table 1
Evolutions of the SE discretization (N_b), number of primal and dual problems solves and errors on mean and variance of the solution (at $x = 0.52$), with h_ξ-refinement iteration and q = 2.

p = 6, N_x = 6). Figure 4 shows the resulting partition of Ω_ξ and surface response of the solution at $x = 0.1$ for q = 1, 3 and 5. It is seen that to satisfy the same error criterion a lower number of FEs is necessary when the stochastic order increases. Specifically, for q = 1, 174 SEs are needed compared to 10 for q = 5. It is also seen that the partition of Ω_ξ is essentially refined in the lower quadrant corresponding to lower values of the viscosity. An asymmetry of the resulting partition of Ω_ξ is also seen for q = 1, denoting the different contributions of ξ_1 and ξ_2 to the uncertainty of the solution as one may have expected from the parameterization in Eq. (51).

Further more, the surface responses in Figure 4 show that the refinement of Ω_ξ takes place in areas where the solution exhibits the steepest dependence with regards to ξ, but also in areas where it is essentially unaffected by the viscosity; this is due to the fact that the refinement is based on a criterion involving all spatial locations: the solution at different spatial locations requires refinement at different places in Ω_ξ.

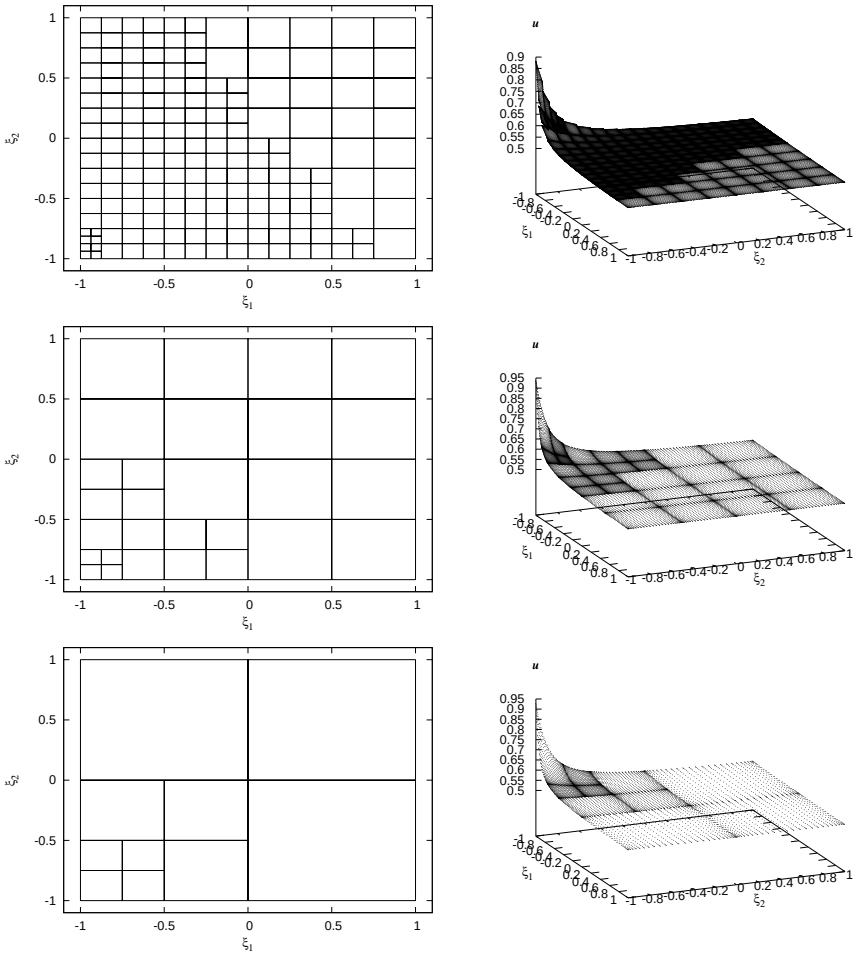

Fig. 4. Partition of Ω_ξ (left) and surface response for $U(\xi)$ at $x = 0.1$ (right) at the end of the isotropic h_ξ-refinement process using $\epsilon = 5.10^{-5}$. Plots correspond to q = 1, 3 and 5 from top to bottom.

5.3 Isotropic $h_{\xi,x}$-refinement

In the previous tests, an isotropic h_ξ-refinement only was applied. However, as discussed previously, the *a posteriori* error estimate incorporate both the stochastic and spatial errors. In fact, it is expected that when lowering μ a finer and finer spatial FE discretization in the neighborhood of $x = 0$ is needed as the solution becomes stiffer and stiffer. Consequently, one may find advantages in adapting the FE discretization to $\Omega_\xi^{(m)}$. This is achieved by introducing an

additional test before applying the isotropic h_ξ-refinement. If the local error $\eta_{l,n}$ is greater than ϵ, the spatial discretization is first checked by computing an estimate of the spatial error $\eta^x_{l,m}$ from

$$\left(\eta^x_{l,m}\right)^2 = \int_{\Omega^{(l)}_x} \left\langle \left[U^h - \Pi^l(U^h)\right]^2 \right\rangle_{\Omega^{(m)}_\xi} \, dx, \tag{60}$$

where $\Pi^l(U^h)$ is the (spatial) Clément interpolant [6] of U^h over the spatial patch defined by the union of the FEs having a common point with the element $\Omega^{(l)}_x$. The order of the Clément interpolant is set to $\mathrm{p}(l,m)+1$. If this estimate of the spatial error is greater than a prescribed second threshold ϵ_x a h_x-refinement is applied to the FE $\Omega^{(l)}_x$ (for the SE $\Omega^{(m)}_\xi$ only), consisting in its partition into two Chebyshev elements of equal size. On the contrary, if $\eta^x_{l,m} < \epsilon_x$ for all $l \in [1, \mathrm{N_b}(m)]$, the h_ξ-refinement is applied as previously.

This strategy is applied to the test problem, with the initial discretization using $\mathrm{N_x} = 6$ identical FEs with $\mathrm{p} = 6$, over 4 equal SEs with $\mathrm{q} = 2$ and a refinement criteria $\epsilon = 10^{-4}$. The partition of Ω at the end of the refinement process is shown in Figure 5. The left plot shows the partition of Ω_ξ and highlights again the need for refinement for the lowest values of the viscosity. The right plot shows the dependence of the refinement of the FE discretization with ξ. Specifically, it is seen that h_x-refinement essentially occurs for the lowest values of the viscosity (*i.e.* when the solution exhibits the steepest spatial evolutions) and in the neighborhood of $x = 0$ as one may have expected.

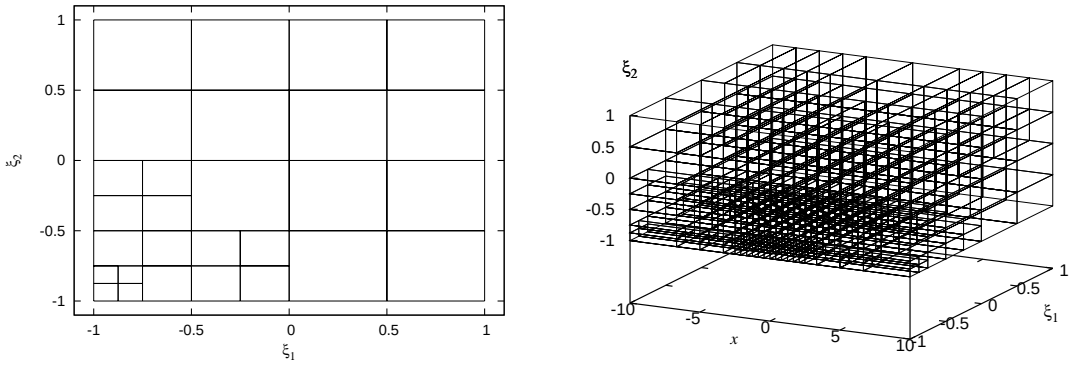

Fig. 5. Partition of Ω_ξ (left) and Ω (right) after the $h_{\xi,x}$-refinement procedure. Numerical parameters are given in the text.

Additional insights about the distribution of the local *a posteriori* error estimate $\eta_{l,m}$ in Ω can be gained examining Figure 6, where plotted is the local error magnitude as spheres. A large sphere corresponds to a large error $\eta_{l,m}$, with a scaling of the spheres' diameter as $d \sim \eta^{0.25}_{l,m}$. As already stated, it is seen that the maximum error occurs around $x = 0$ and that it decreases very quickly as one gets away from that location. This plot clearly exemplifies the

h-refinement strategy: divide elements where a large error occurs to make the error magnitude below the prescribed tolerance $\eta_{l,m}$.

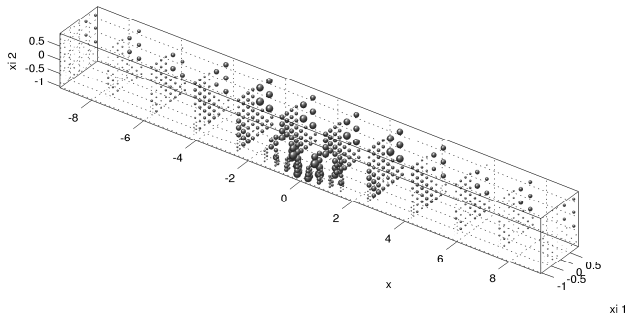

Fig. 6. Distribution of the local *a posteriori* error estimate $\eta_{l,m}$ after $h_{\xi,x}$-refinement. The spheres' diameter d scales as $d \sim \eta_{l,m}^{0.25}$.

We present in Figure 7 the expectation (left) and variance (right) of the approximate solution U^h after refinement as a function of x. The plot of the expectation $\left\langle U^h \right\rangle_{\Omega_\xi}$ is also compared with the deterministic solution $u(x)$ for the mean viscosity $\mu_0 = 1$. This deterministic solution has for expression:

$$u(x; \mu = 1) = \frac{1}{2}\left[1 + \tanh\frac{x}{4}\right]. \tag{61}$$

It is seen that the expected solution also has an hyperbolic tangent-like profile but is not equal to the deterministic solution: the differences are due to the non-linearities of the Burgers' equation. The right plot in Figure 7 depicts the solution variance $\sigma^2(U^h)$. The boundary conditions being deterministic the variance vanishes at x^- and x^+. The uncertainty in the viscosity produces a symmetric variance with regards to $x = 0$ as it only affects the steepness of the hyperbolic tangent-like profile since

$$U(x, \xi) \approx \frac{1}{2}\left[1 + \tanh\frac{x}{4\,\mu(\xi)}\right]. \tag{62}$$

Also, due to the selected boundary conditions, we have at the center of the spatial domain $U(\xi) = (u^- + u^+)/2 = 1/2$ almost surely, provided that $\mu(\xi) > 0$. Therefore, the variance of U^h vanishes at $x = 0$ as shown in Figure 7.

The probability density functions of U^h, together with the solution's quantiles, are reported in Figure 8 as functions of x. The quantiles are defined as the level $u(Q)$, for $Q \in]0, 1[$, such that the probability of $U^h(x) < u$ is equal to Q. The plot of the pdf shows dramatic changes with x. For $x = x^-$ the pdf is a Dirac of unit mass (no-uncertainty); then when x increases the pdf evolves from a sharp lower tail distribution to a long lower tail distribution. At $x = 0$ it is again a Dirac (no-uncertainty). For x increasing further to x^+ the opposite evolution is observed (due to the central symmetry of the settings). Note that

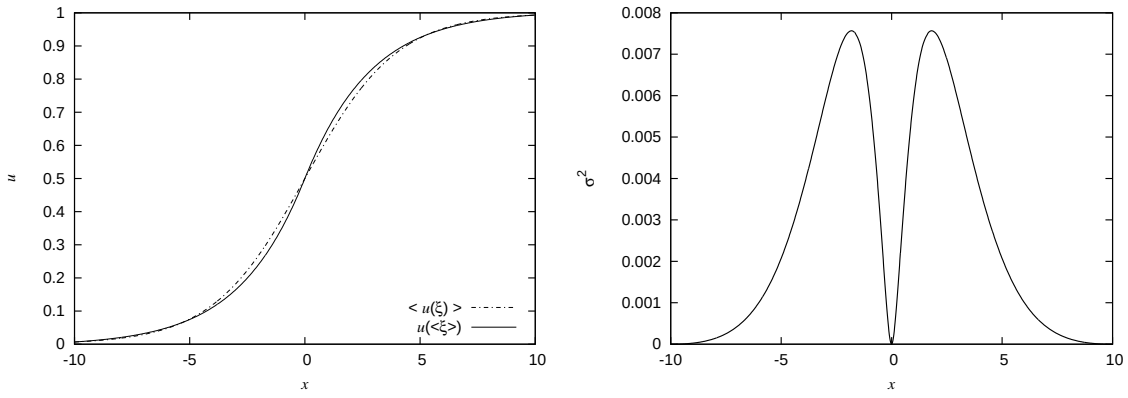

Fig. 7. Expectation (left) and variance (right) of the approximate solution $U^h(x,\xi)$ at the end of the $h_{\xi,x}$-refinement process.

the distribution of the solution is bounded since U almost surely $\in [u^-, 1/2]$ for $x \leq 0$ and U almost surely $\in [1/2, u^+]$ for $x \geq 0$. The quantiles reflect the complexity of the distribution with important changes with x of the spacing between quantiles.

To further illustrate the need of refinement to properly capture the solution distribution, we present in Figure 9 the convergence of the pdf of U^h at $x = 0.52$ along the $h_{\xi,x}$-refinement process. The left plot shows the pdf in linear-log scales to appreciate the improvement in the tails of the distribution, while the right plot in linear-linear scales shows the improvement in the high density region. It is seen that during the first iterations of the refinement process the pdf presents under-estimated right-tails and some spurious oscillations, which are due to discontinuities of the approximate solution across SEs boundaries.

5.4 Anisotropic h/q-refinement

In the previous tests, an isotropic h-refinement was used in the stochastic domain. As a result, each refined SE is split into 2^{N} SEs. For large N this simple procedure quickly results in a prohibitively large number of SEs. Instead, one finds advantage in splitting $\Omega_\xi^{(m)}$ only along the stochastic directions yielding the largest error reduction. Obviously, the *a posteriori* error estimate does not provide enough information to decide along which directions $\Omega_\xi^{(m)}$ should be split: an anisotropic error estimator is necessary to this end. In the absence of such estimator, we rely on a criterion, inspired from [17, 27], which is based on the relative contributions of each stochastic directions to the local variance. The local variance is defined as

$$\sigma^2_{\Omega_\xi^{(m)}}(U) = \left\langle \left[U - \langle U \rangle_{\Omega_\xi^{(m)}} \right]^2 \right\rangle_{\Omega_\xi^{(m)}} . \tag{63}$$

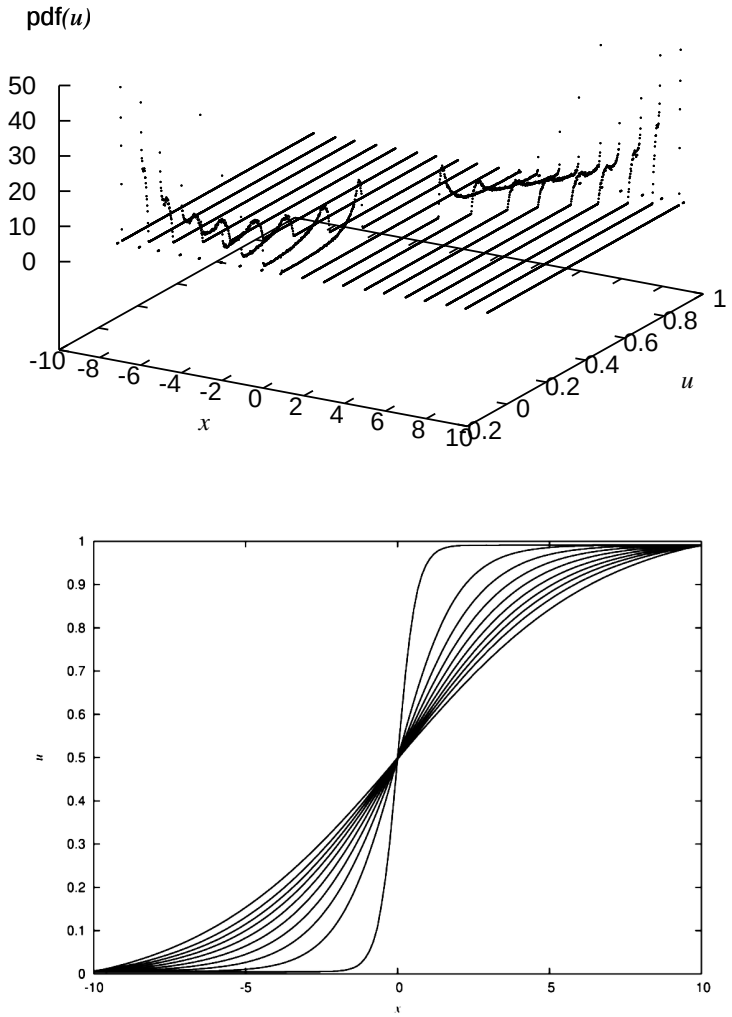

Fig. 8. Top: pdf of the approximate solution U^h as a function of x at the end of the $h_{\xi,x}$-refinement. The pdf-axis is truncated for clarity. Bottom: quantiles $u(Q)$ of the solution, as a function of x, for $Q = 0.05$ to 0.95 with constant increment $\Delta Q = 0.1$.

Since the stochastic expansion of U over $\Omega_\xi^{(m)}$ writes as

$$U(\xi \in \Omega_\xi^{(m)}) = \sum_{k=0}^{\mathrm{P}(m)} u_k^{(m)} \Psi_k^{(m)}(\xi),$$

and because by convention $\Psi_k^{(m)} = 1$ for $k = 0$ (*i.e.* mode 0 is the mean mode), the local variance writes:

$$\sigma^2_{\Omega_\xi^{(m)}}(U) = \sum_{k=1}^{\mathrm{P}(m)} \left(u_k^{(m)}\right)^2 \left\langle {\Psi_k^{(m)}}^2 \right\rangle_{\Omega_\xi^{(m)}}, \tag{64}$$

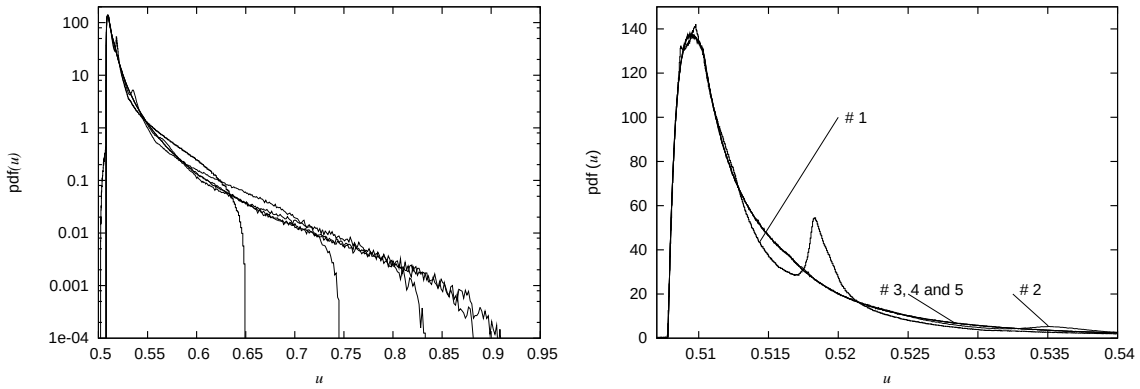

Fig. 9. Probability density function at $x = 0.52$ for different steps of the $h_{\xi,x}$-refinement process. Linear-log plot (left) and linear-linear plot (right).

and we define

$$\sigma^2_{\Omega_\xi^{(m)}\times\Omega_x^{(l)}}(U) = \sum_{k=1}^{\mathrm{P}(m)} \left\langle {\Psi_k^{(m)}}^2 \right\rangle_{\Omega_\xi^{(m)}} \int_{\Omega_x^{(l)}} \left(u_k^{(m)}(x)\right)^2 dx. \tag{65}$$

It is seen that the integral of the local variance on the FE $\Omega_x^{(l)}$ is a weighted sum of the integral of the squared stochastic expansion coefficients over the FE. The idea is thus to define, for each direction $i = 1, \ldots, \mathrm{N}$, the contribution of the polynomial of degree $\mathrm{q}(m)$ in ξ_i to this variance integrated on $\Omega_x^{(l)}$. This contribution is denoted $\sigma^2_{l,m}(U; i, \mathrm{q}(m))$. Using the respective contributions of each direction, it is decided that $\Omega_\xi^{(m)}$ has to be split along the i-th stochastic direction if the following test is satisfied for at least one FE:

$$\frac{\sigma^2_{l,m}(U; i, \mathrm{q}(m))}{\sum_{i=1}^{\mathrm{N}} \sigma^2_{l,m}(U; i, \mathrm{q}(m))} \geq \epsilon_2. \tag{66}$$

where $0 < \epsilon_2 < 1$ is an additional threshold parameter. If none of the stochastic directions satisfies the previous test, it is on the contrary decided to increment by one unit the stochastic expansion order $\mathrm{q}(m)$ over $\Omega_\xi^{(m)}$.

The anisotropic h/p-refinement strategy now follows the general algorithm:

1. solve the primal and dual problems for the current approximation space $\mathcal{V}^h$; get U^h and Z^h.
2. Solve the adjoint problem in the enriched space $\mathcal{V}^{\widetilde{h}}$; get $\widetilde{Z}$.
3. Compute the local error $\eta_{l,m}$ from Eq. (46) for $m = 1, \ldots, \mathrm{N_b}$, $l = 1, \ldots, \mathrm{N_x}(m)$. If $\eta_{l,m} < \epsilon$ for $m = 1, \ldots, \mathrm{N_b}$, $l = 1, \ldots, \mathrm{N_x}(m)$, then end computation.
4. For $m = 1, \ldots, \mathrm{N_b}$ and $l = 1, \ldots, \mathrm{N_x}(m)$
   If $\eta_{l,m} > \epsilon$:
   a. Compute the estimate of the spatial error $\eta^x_{l,m}$ using Eq. (60).
   b. If $\eta^x_{l,m} > \epsilon_x$, mark element for h_x-refinement.

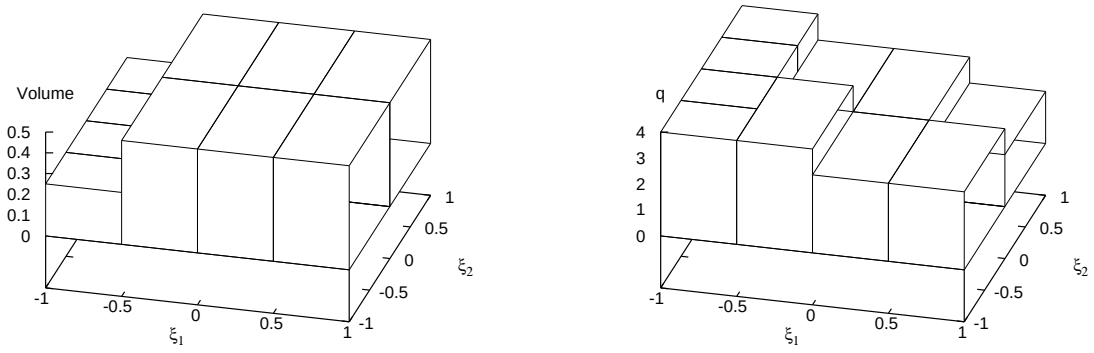

Fig. 10. Volume $\left|\Omega_\xi^{(m)}\right|$ and corresponding stochastic expansion order q over the partition of Ω_ξ. Anisotropic h/q-refinement.

c. If the element has not been marked for h_x-refinement,
   a) Compute the directional variances.
   b) For $i = 1, \ldots, \mathrm{N}$ if the directional variance is greater than ϵ_2 then mark element $\Omega_\xi^{(m)}$ for h_ξ-refinement in direction i.

5. For $m = 1, \ldots, \mathrm{N_b}$: if $\Omega_\xi^{(m)}$ has not been marked for some h_ξ-refinement, and none of the elements $\Omega_\xi^{(m)} \times \Omega_x^{(l)}$, $l = 1, \ldots, \mathrm{N_x}(m)$, are marked for h_x-refinement but there exists at least one $l \in [1, \mathrm{N_x}(m)]$ such that $\eta_{l,m} > \epsilon$, then increase $\mathrm{q}(m)$ by one.
6. Construct the refined approximation space and restart from 1.

This refinement scheme has been successfully applied to the test problem, with $\mu_1 = 0.82$ and $\mu_2 = 0.16$. The viscosity parameterization was changed to increase the contribution of the first direction compared to the second to the solution uncertainty. Note that the pdf of μ is affected by this change of the parameterization, but the uncertainty range is kept constant. For illustration purposes, we present in Figure 10 an example of the partition of the stochastic space into SEs with variable stochastic expansion orders. The initial discretization involves $\mathrm{N_b} = 4$ equal SEs with $\mathrm{q} = 2$. At the first iteration, all SEs were split isotropically, the expansion order being kept constant. At the second iteration, the SEs with boundary at $\xi_1 = -1$ were further refined but in the ξ_1 direction only. For the following iterations, no further h_ξ-refinement was required while some SEs still have a significant estimated error: it yielded increase in the stochastic expansion order $\mathrm{q}(m)$. Again, the final expansion order is the greatest for the SEs with $\xi_1 = -1$ and/or $\xi_2 = -1$ boundaries (where viscosity is small), and is the lowest for the SE having boundary $\xi_1 = 1$ and $\xi_2 = 1$ where q has been kept constant.

To conclude this series of tests, an additional uncertainty source is considered by taking the left boundary condition as random, U^-. The random boundary condition is assumed independent of the viscosity value and consequently parameterized using an additional random variable ξ_3. The complete uncertainty settings are:

$$\mu(\xi) = 1 + 0.5\,\xi_1 + 0.05\,\xi_2, \quad U^-(\xi) = u_0^- + u'\,\xi_3, \tag{67}$$

with u_0^- given by Eq. (52) and $u' = 5.\,10^{-4}$. This low value of u' is selected as it is known that small perturbations of the boundary condition leads to $O(1)$ changes in the solution of the Burgers' equation (see [31]). This is due to the "supersensitivity" of the transition layer location with the boundary condition: the low variability in U^- will result in large variability of the solution but essentially around the center of the spatial domain and not in the neighborhood of x^- where the solution variability is low. This problem is thus well suited to test the effectiveness of the *a posteriori* error methodology in providing correct local error estimators. Moreover, as the sensitivity of the solution with regards to U^- increases when the viscosity is lowered, a finer partition of Ω_ξ is expected for low values of ξ_1, while the contribution of ξ_2 will be less as seen from Eq.(67).

The spatial discretization ($\mathrm{N_x} = 20$, $\mathrm{p} = 6$) and stochastic orders q being held fixed, we proceed with the *a posteriori* error based anisotropic h_ξ-refinement scheme described above. The target precision is set to $\epsilon_\eta = 0.001$. In Figure 11 we show the reduction of the *a posteriori* error η along the refinement process for orders $\mathrm{q} = 1$ and 2. The evolution of the error estimate for a uniform refinement of the stochastic space is also reported for comparison. Because the stochastic space now has 3 dimensions, the increase in number of SEs for the uniform refinement is seen to be dramatically large for a low resulting reduction of the *a posteriori* error. On the contrary, using the local error estimate to guide the refinement process is seen to significantly improve the error reduction with the number of SEs. It is also remarked that the anisotropic refinement requires 3 iterations to achieve the prescribed precision for $\mathrm{q} = 1$, while only 2 iterations are needed for $\mathrm{q} = 2$.

Figure 12 depicts the partition of the stochastic space at the end of the h_ξ-refinement process. The initial partition uses $\mathrm{N_b} = 2^{\mathrm{N}} = 8$ identical SEs. In fact, the anisotropic h_ξ-refinement process never requires refinement along the second dimension ξ_2: the plots of Figure 12 thus show the partition of Ω_ξ in a plane where ξ_2 is constant. The independence of the partition with regards to ξ_2 denotes the capability of the proposed scheme to detect the weak influence of ξ_2 on the solution. On the contrary, it is seen that for fixed ξ_2 and ξ_3 a finer division of Ω_ξ along the first direction is necessary when ξ_1 decreases,

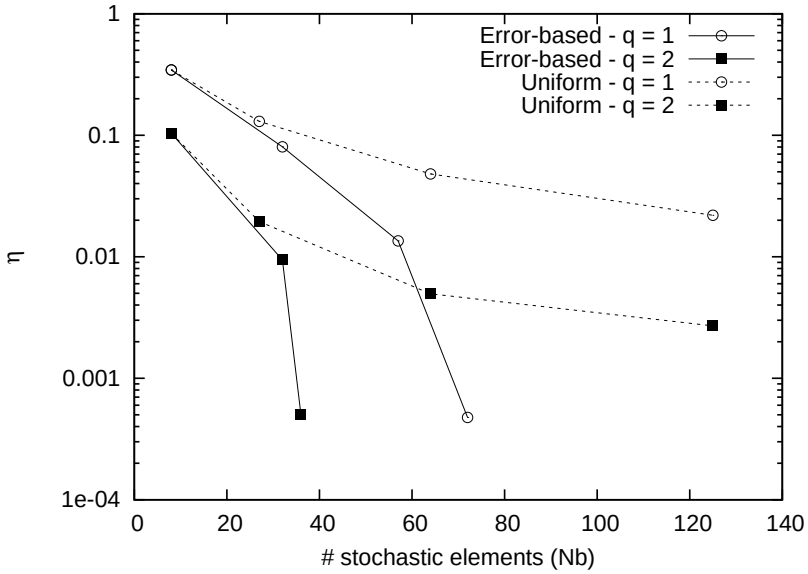

Fig. 11. Reduction of the *a posteriori* error estimate η with the number N_b of stochastic elements involves in the partition of Ω_ξ. Plotted are the results for the anisotropic h_ξ-refinement procedure (labeled Error-based) and uniform refinement, using q = 1 and 2 as indicated.

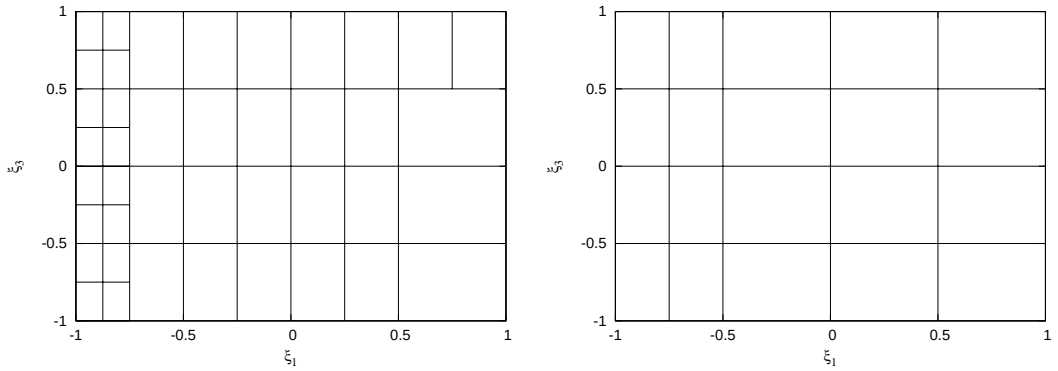

Fig. 12. Partition of Ω_ξ at the end of the anisotropic h_ξ-refinement process in a plane corresponding to constant ξ_2. Left q = 1 and right q = 2.

because of the steeper behavior of the solution when the viscosity decreases. In contrast, for fixed ξ_1 and ξ_2 the partition is uniform along the third direction, but is finer for low viscosity and q = 1, as one may have anticipated from the behavior of the Burgers' solution.

To conclude these tests, we show in Figure 13 the variance of the stochastic solution along the spatial domain, for the two stochastic orders q = 1 and 2, at the end of the anisotropic refinement process. The effect of the uncertain boundary condition on the solution variance can be appreciated through comparison with the result reported in Figure 7. Specifically, the variance of the solution at the center of the spatial domain is now different from zero. It is seen

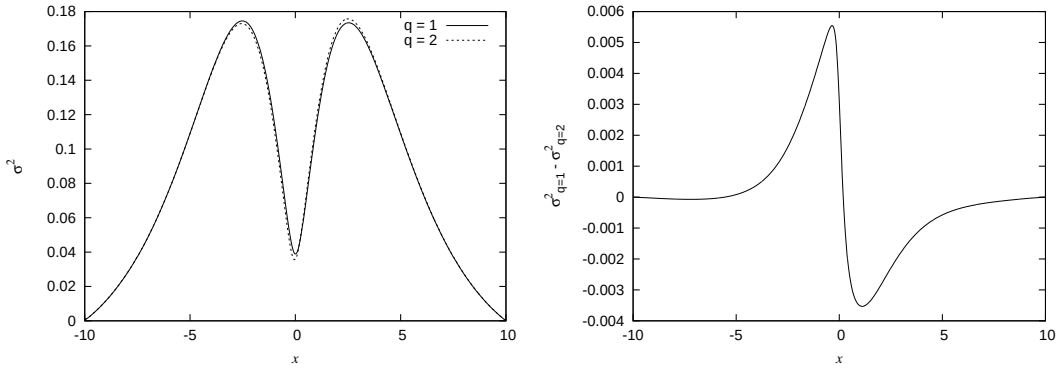

Fig. 13. Left : comparison of the variances in $U(\xi)$ as a function of x for stochastic expansion orders q = 1 and q = 2 at the end of the anisotropic h_ξ-refinement process. Right : difference of the two variances predicted for q = 1 and q = 2.

that even so both orders leads to similar estimated error, small but noticeable differences are visible in the spatial distribution of the solution variance. These difference in terms of predicted variance can be better appreciated from the right plot in Figure 13 where the differences for q = 1 and q = 2 are plotted.

6 Concluding remarks

A dual-based *a posteriori* error analysis has been proposed in the context of stochastic finite element methods with stochastic discretization involving piecewise continuous orthogonal polynomials approximations. The error estimation involves the resolution of a linear stochastic dual problem, which computational cost is deemed negligible compared to the primal problem (provided the latter is non-linear). Numerical tests on the uncertain Burgers' equation have demonstrated the effectiveness of the methodology in providing relevant error estimates that can be localized in the spatial and stochastic domain.

The principal limitation of the proposed method is the lack of resulting information regarding the structure of the estimated error. Specifically, the respective contributions of the spatial and stochastic approximations to the estimated error are not accessible. At a finer level, the error estimator does not allow for the discrimination between the relative contributions of the stochastic directions to the overall error. We believe this is the most severe limitation in view of anisotropic refinement of the stochastic approximation space required to treat problems with high dimensional uncertainty germs. However, we consider that the proposed methodology constitutes a significant improvement compared to error indicators previously proposed in the stochastic context [17, 18, 27], which were based on the spectrum of the local stochastic expansion.

Several potential improvements of the refinement strategy have been identified throughout this work. It includes the derivation of rigorous and efficient anisotropic error estimators for high order approximation schemes. Another area of potential application of the *a posteriori* estimator is the coarsening of the approximation space in view of application to, say, unsteady flows. Both of these developments are the subject of on-going work.

References

[1] M. Abramowitz and I. Stegun. *Handbook of mathematical functions.* Dover, 1970.

[2] I. Babuška and A.D. Miller. A feedback finite element method with a posteriori error estimation. *Comp. Methods Appl. Mech. Engrg.*, 61:1–40, 1987.

[3] I. Babuška and W.C. Rheinboldt. A posteriori error estimates for the finite element method. *Int. J. Numer. Meth. Engrg.*, 12:1597–1615, 1978.

[4] R. Becker and R. Rannacher. An optimal control approach to a posteriori error estimation in finite element methods. *Acta Numer.*, 10:1–102, 2001.

[5] R.H. Cameron and W.T. Martin. The orthogonal development of nonlinear functionals in series of Fourier-Hermite functionals. *Ann. Math.*, 48:385–392, 1947.

[6] P. Clément. Approximation by finite element functions using local regularization. *Rev. Française Automat. Inform. Rech. Opér., Sér. Rouge Anal. Numér.*, 9(R-2):77–84, 1975.

[7] B. Debusschere, H.N. Najm, A. Matta, O.M. Knio, R.G. Ghanem, and O.P. Le Maître. Protein labelling reactions in electrochemical flow: numerical simulation and uncertainty propagation. *Phys. Fluids*, 15(8):2238–2250, 2003.

[8] R. Ghanem and S. Dham. Stochastic finite element analysis for multiphase flow in heterogeneous porous media. *Transp. Porous Media*, 32:239–262, 1998.

[9] R.G. Ghanem. Probabilistic characterization of transport in heterogeneous media. *Comp. Meth. App. Mech. Eng.*, 158:199–220, 1998.

[10] R.G. Ghanem and P.D. Spanos. *Stochastic finite elements. A spectral approach.* Dover Publications, Inc., rev. edition, 1991. 222 p.

[11] V. Heuveline and R. Rannacher. Duality-base adaptivity in the *hp*-finite element method. *J. Numer. Math.*, 12(2):95–113, 2003.

[12] T.D. Hien and M. Kleiber. Stochastic finite element modeling in linear transcient heat transfer. *Comp. Met. App. Mech. Eng.*, 144:111–124, 1997.

[13] M. Kaminski and T.D. Hien. Stochastic finite element modeling of transcient heat transfer in layered composites. *Int. Com. Heat and Mass Trans.*, 26(6):801–810, 1999.

[14] O.M. Knio and O.P. Le Maître. Uncertainty propagation in CFD using polynomial chaos decomposition. *Fluid Dyn. Res.*, 38:616–640, 2006.

[15] O.P. Le Maître, O.M. Knio, H.N. Najm, and R.G. Ghanem. A stochastic projection method for fluid flow. i. basic formulation. *J. Comp. Phyics*, 173:481–511, 2001.

[16] O.P. Le Maître, O.M. Knio, H.N. Najm, and R.G. Ghanem. Uncertainty propagation using Wiener-Haar expansions. *J. Comp. Phys.*, 197(1):28–57, 2004.

[17] O.P. Le Maître, H.N. Najm, R.G. Ghanem, and O.M. Knio. Multi-resolution analysis of Wiener-type uncertainty propagation schemes. *J. Comp. Phys.*, 197(2):502–531, 2004.

[18] O.P. Le Maître, H.N. Najm, P.P. Pébay, R.G. Ghanem, and O. Knio. Multi-resolution analysis for uncertainty quantification in chemical systems. *SIAM J. Sci. Comp.*, 2006. in press.

[19] O.P. Le Maître, M.T. Reagan, O.M. Knio, H.N. Najm, and R.G. Ghanem. A stochastic projection method for fluid flow. ii. random process. *J. Comp. Phys.*, 181(1):9–44, 2002.

[20] O.P. Le Maître, M.T. Reagan, B. Debusschere, H.N. Najm, R.G. Ghanem, and O.M. Knio. Natural convection in a closed cavity under stochastic, non-Boussinesq conditions. *J. Sci. Comp.*, 26(2):375–394, 2004.

[21] L. Mathelin, M.Y. Hussaini, and T.A. Zang. Stochastic approaches to uncertainty quantification in CFD simulations. *Num. Algo.*, 38(1):209–239, 2005.

[22] S. Micheletti, S. Perotto, and M. Picasso. Stabilized finite elements on anisotropic meshes: a priori error estimates for the advection-diffusion and the stokes problems. *SIAM J. Numer. Anal.*, 41(3):1131–1162, 2003.

[23] J. Peraire, J. Peiró, and K. Morgan. Adaptive remeshing for three-dimensional compressible flow computations. *J. Comp. Phys.*, 103(2):269–285, 1992.

[24] M.T. Reagan, H.N. Najm, R.G. Ghanem, and O.M. Knio. Uncertainty quantification in reacting flow simulations through non-intrusive spectral projection. *Combustion and Flames*, 132:545–555, 2003.

[25] G.I. Schuëller. Computational stochastic mechanics - recent advances. *Computers and Structures*, 79:2225–2234, 2001.

[26] R.W. Walters and L. Huyse. Uncertainty analysis for fluid mechanics with applications. Technical report, NASA CR-2002-211449, 2002.

[27] X. Wan and G.E. Karniadakis. An adaptive multi-element generalized polynomial chaos method for stochastic diffential equations. *J. Comp. Phys.*, 209:617–642, 2005.

[28] N. Wiener. The homogeneous chaos. *Amer. J. Math.*, 60(4):897–936, 1938.

[29] D. Xiu and G.E. Karniadakis. The Wiener-Askey polynomial chaos for stochastic differential equations. *SIAM J. Sci. Comp.*, 24(2):619–644, 2002.

[30] D. Xiu and G.E. Karniadakis. Modeling uncertainty in flow simulations

via generalized polynomial chaos. *J. Comp. Phys.*, 187:137–167, 2003.
[31] D. Xiu and G.E. Karniadakis. Supersensitivity due to uncertain boundary conditions. *Int. J. Numer. Meth. Engng.*, 61(12):2114–2138, 2004.